J. Fluid Mech. (1983), *vol.* 129, *pp.* 55–75
Printed in Great Britain

Laminar natural convection from a horizontal plate and the influence of plate-edge extensions

By R. J. GOLDSTEIN AND KEI-SHUN LAU
Department of Mechanical Engineering, University of Minnesota, Minneapolis, Minnesota 55455

(Received 10 June 1982)

Laminar natural convection from a horizontal plate is studied by a finite-difference analysis and by experiments for Rayleigh numbers from 10 to 10^4. The plate with uniform surface temperature or concentration on one side and insulated on the other is situated in an 'infinite' fluid medium. The buoyancy near the surface is directed either outward or inward normal to the active surface – equivalent to a heated plate facing upward or downward. The effect of insulated vertical and horizontal extensions to the plate are also examined.

Finite-difference solutions are obtained for a heated strip in a two-dimensional domain for a Prandtl number of 0·7. Mass-transfer experiments are performed with square naphthalene plates in air. Both numerical and experimental results justify a $\frac{1}{5}$-power law in the present range of Rayleigh number – i.e. Nusselt number or Sherwood number proportional to the Rayleigh number raised to the $\frac{1}{5}$ power. The horizontal extensions cause a limited reduction in the transfer rate for the plate generating 'outward buoyancy', and a larger reduction with 'inward buoyancy'. The vertical walls block the fluid flow directly, and thus greatly lower the transfer rate with either outward or inward buoyancy.

1. Introduction

The density of fluid near a solid surface can be different from that of the surrounding fluid owing to heat transfer, mass transfer or other processes. The buoyancy forces created by this density difference in a gravitational or other body force field generate a natural convection flow. The scope of the present study, limited to laminar flow, is classified by six geometric configurations listed on table 1 and illustrated in figure 1. Geometry 0 is a simple plate in which the buoyancy force is outward normal to its active surface. This might be a heated horizontal plate facing upward or a horizontal subliming naphthalene surface in air facing downward. In such an event, fluid is drawn from edges and then moves away from the surface owing to the outward buoyancy. Geometry I is a similar plate in which the buoyancy forces are directed inward, normal to the surface. Examples are a heated plate facing downward and a naphthalene plate in air facing upward. With this geometry, fluid is drawn inward toward the centre of the surface and moves outward toward the edges. Geometries 0H, 0V, IH and IV refer to horizontal (H) and vertical (V) extensions on the plate edges of geometries 0 and I.

The present laminar natural convection is characterized by the dimensionless parameters: Prandtl number $Pr = \nu/\alpha$ and Rayleigh number $Ra = ga^3(\rho_\infty - \rho_s)/\nu\alpha\rho_\infty$ in the heat-transfer problem; or Schmidt number $Sc = \nu/D$ and Rayleigh number $Ra_m = ga^3(\rho_\infty - \rho_s)/\nu D\rho_\infty$ in the mass-transfer problem. The variable ν is kinematic viscosity, α is thermal diffusivity, g is gravitational acceleration, a is characteristic

Geometry	Mass-transfer experiments on square naphthalene plates in air	Finite-difference solution for the laminar-flow two-dimensional heat-transfer problem in fluids with a positive coefficient of thermal expansion
0 – simple plate with buoyancy force outward normal to its active surface	Simple naphthalene plate facing downward (extension/side < 0·06)	Simple heated plate facing upward; extension/side = $\frac{1}{20}$
0H – geometry 0 with horizontal extensions at plate edges	Downward-facing naphthalene plate with horizontal extensions; extension/side = $\frac{1}{2}$ (i.e. extension/half-width = 1)	Upward-facing plate with horizontal adiabatic extensions extension/side = $\frac{1}{4}$, $\frac{1}{2}$, 1, 2
0V – geometry 0 with vertical walls at plate edges	Downward-facing naphthalene plate with vertical walls; wall/side = 1, 2, 3	Upward-facing heated plate with vertical adiabatic walls; wall/side = $\frac{3}{40}$, $\frac{1}{4}$, $\frac{1}{2}$, 1, 2
I – simple plate with buoyancy force inward normal to its active surface	Simple naphthalene plate facing upward; extension/side < 0·06	Simple heated plate facing downward; extension/side = $\frac{1}{20}$
IH – geometry I with horizontal extensions at plate edges	Upward-facing naphthalene plate with horizontal extensions; extension/side = $\frac{1}{2}$	Downward-facing heated plate with horizontal adiabatic extensions; extension/side = $\frac{1}{4}$, $\frac{1}{2}$, 2
IV – geometry I with vertical walls at plate edges	Upward-facing naphthalene plate with vertical walls; wall/side = 1	Downward-facing heated plate with vertical adiabatic walls; wall/side = $\frac{1}{2}$, 1

TABLE 1. Scope of present study

length, ρ_∞ is the fluid density far from the surface, ρ_s is the fluid density (generally assumed constant) adjacent to the surface. and D is the binary diffusivity of the two species (e.g. naphthalene vapour in air). The heat-transfer coefficient in dimensionless form is the Nusselt number $Nu = a\dot{q}/k(T_s - T_\infty)$ and the dimensionless mass-transfer coefficient is the Sherwood number $Sh = a\dot{m}/D\rho_s(C_s - C_\infty)$, where $\dot{q}$ is heat flux, k is thermal conductivity, T is temperature, $\dot{m}$ is mass flux, C is the mass fraction of the fluid component supplied from the surface, subscript s refers to surface, and subscript ∞ refers to a region far from the surface.

Different characteristic lengths were used in previous studies. In order to compare plates of various shapes, Goldstein, Sparrow & Jones (1973) proposed a lengthscale a defined as the active surface area divided by its perimeter (i.e. $a = \frac{1}{2} \times$ width for an infinite strip and $a = \frac{1}{4} \times$ side for a square). Lloyd & Moran (1974) found that this dimension helped correlate their results as well. This characteristic length is used in the present study.

Experimental studies on geometry 0 are summarized in table 2. Heat-transfer results can be found in Fishenden & Saunders (1950), Bosworth (1952), Mikheyev (1968) and Al-Arabi & El-Riedy (1976). Electrochemical experiments were performed by Wragg (1968), Wragg & Loomba (1970) and Lloyd & Moran (1974). In the

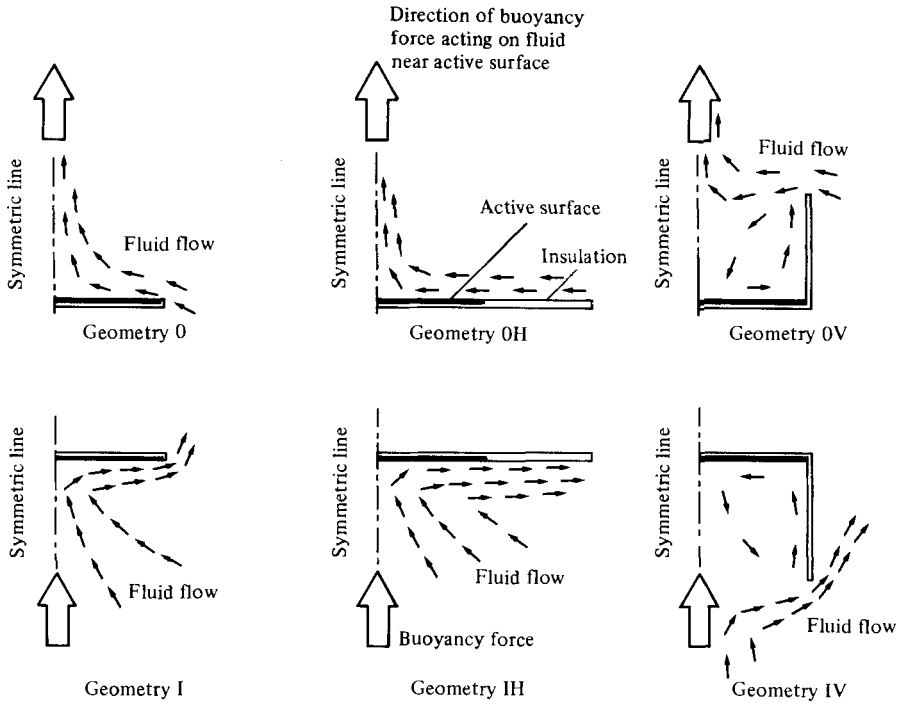

FIGURE 1. The geometries of horizontal plates and plate-edge extensions in the present study.

aforementioned results, the data were generally presented as a $\frac{1}{4}$-power correlation ($Nu \propto Ra^{\frac{1}{4}}$ or $Sh \propto Ra_m^{\frac{1}{4}}$) in the laminar regime and $\frac{1}{3}$-power ($Nu \propto Ra^{\frac{1}{3}}$ or $Sh \propto Ra_m^{\frac{1}{3}}$) in the turbulent regime. Bandrowski & Rybski (1976) found a power of 0·222. Goldstein *et al.* (1973) correlated their data with $\frac{1}{6}$- and $\frac{1}{4}$-power relationships depending on the range of Ra. With only one curve for the data from this reference for Ra between 10 and 10^4, a power of 0·211 can be used.

The schlieren photographs in Rotem & Claassen (1969) and the interferograms in Pera & Gebhart (1973) support the concept of a boundary layer with geometry 0. Boundary-layer solutions that have been obtained for this geometry are listed in table 3. For a heated semi-infinite surface, Levy & Schenectady (1955) obtained an integral solution. Stewartson (1958), Rotem & Claassen and Pera & Gebhart found similarity solutions. Assuming that the flow paths were parallel, Ackroyd (1976) obtained a heat-transfer solution for rectangular plates. Extending Ackroyd's solution method, Zakerullah & Ackroyd (1979) found a similarity solution for a disk. In the mass-transfer problem the flow velocity is not zero at the source surface but depends on the mass fraction of the fluid. Bandrowski & Rybski (1976) obtained similarity solutions for uniform mass fraction at the wall. Kerr (1980) improved their results. These solutions indicate that the normal velocity at the surface has no significant effect on the mass-transfer rate with the small fraction of naphthalene vapour present in most sublimation studies. In the boundary-layer solutions the $\frac{1}{5}$-power law was found.

The discrepancy in the power law between theory and experiments is well known. It was believed that the interaction of the flow in the middle of a finite plate caused deviation from boundary-layer flow. Ackroyd (1976) calculated that the change of air properties raised the power from $\frac{1}{5}$ to $\frac{1}{4}$ when the temperature gradient was raised from zero to twice the reference absolute temperature. This temperature difference,

Reference	$Nu = \text{C1}\ Ra^{\text{C2}}$ or $Sh = \text{C1}\ Ra_m^{\text{C2}}$ C1	C2	Range of Ra or Ra_m	Experimental techniques
Fishenden & Saunders (1950)	0·38	$\frac{1}{4}$	$1{\cdot}6 \times 10^3$–$1{\cdot}6 \times 10^6$	Heated square plate in air, $Pr \simeq 0{\cdot}7$
Bosworth (1952)	0·50	$\frac{1}{4}$	Laminar	Square plate, unknown fluid, and Pr, heat transfer
Mikheyev (1968)	0·50	$\frac{1}{4}$	$Ra > 7{\cdot}8$	Square plate, unknown fluid and Pr, heat transfer
	0·64	$\frac{1}{8}$	$Ra < 7{\cdot}8$	
Wragg (1968)	0·45	$\frac{1}{4}$	$1{\cdot}6 \times 10^2$–$3{\cdot}9 \times 10^5$	Electrochemical experiment on disk, $Sc \simeq 2300$
Bandrowski & Rybski (1976)	0·69	0·222	$3{\cdot}0 \times 10^3$–$2{\cdot}5 \times 10^5$	Rectangular naphthalene plate in air, $Sc \simeq 2{\cdot}5$
	0·87	$\frac{1}{5}$		Force the above correlation to $\frac{1}{5}$ power
Wragg & Loomba (1970)	0·51	$\frac{1}{4}$	$4{\cdot}7 \times 10^2$–$4{\cdot}7 \times 10^5$	Electrochemical experiment on disk, $Sc \simeq 2300$
Goldstein *et al.* (1973)	0·59	$\frac{1}{4}$	2×10^2–10^4	Circular, square and rectangular naphthalene plates in air, $Sc \approx 2{\cdot}5$
	0·96	$\frac{1}{6}$	1–2×10^2	
	0·783	0·211	10–10^4	Present curve fit for their data
	0·834	$\frac{1}{5}$		Force the above correlation to $\frac{1}{5}$ power
Lloyd & Moran (1974)	0·54	$\frac{1}{4}$	2×10^4–8×10^6	Electrochemical experiment on circular, square, triangular and rectangular plates, $Sc \approx 2200$
Al-Arabi & El-Riedy (1976)	0·50	$\frac{1}{4}$	2×10^5–8×10^6	Heated, square, circular and rectangular plates in air, $Pr \approx 0{\cdot}7$
Present experiment	0·766	0·195	10–$4{\cdot}8 \times 10^3$	Square naphthalene plate in air, $Sc \approx 2{\cdot}5$
	0·746	$\frac{1}{5}$		Force the above correlation to $\frac{1}{5}$ power

TABLE 2. Experiments on simple plate with buoyancy outward normal to its active surface (geometry 0).

however, is much higher than in most experiments, and it cannot explain the mass-transfer experiments. Recently, Ishiguro *et al.* (1978) presented a numerical and experimental result for an infinite strip. Their results seemed to indicate a $\frac{1}{5}$-power region in the lower range of Rayleigh number. Beginning at Rayleigh number about 4×10^4, the power changed gradually from $\frac{1}{5}$ to $\frac{1}{3}$.

Experimental results for geometry I are summarized in table 4. The data of Fishenden & Saunders (1950) were fitted to a $\frac{1}{4}$-power though a $\frac{1}{5}$-power law, which would be appropriate. Experiments by Kadambi & Drake (1960), Birkebak & Abdulkadir (1970), Fujii & Imura (1972), Aihara, Yamada & Endo (1972) and Restrep & Glicksman (1974) justified the existence of boundary-layer flow and indicated a $\frac{1}{5}$-power correlation. Recently Faw & Dullforce (1981) used holographic interferometry to study a downward-facing heated plate for Rayleigh numbers between 5×10^3 and 2×10^5. The temperature distributions found in the experiment

	$Nu = \text{C1}\ Ra^{\text{C2}}$ or $Sh = \text{C1}\ Ra_{\text{m}}^{\text{C2}}$		
Reference	C1	C2	Solution method
Levy & Schenectady (1955)	0·620	$\frac{1}{5}$	Integral method, high Pr, heat transfer from semi-infinite plate
Stewartson (1958)	0·637	$\frac{1}{5}$	Similarity solution, $Pr = 0{\cdot}72$, heat transfer from semi-infinite plate
Rotem & Claassen (1969)	0·639	$\frac{1}{5}$	Similarity solution, $Pr = 0{\cdot}72$, heat transfer from semi-infinite plate
Pera & Gebhart (1973)	0·646	$\frac{1}{5}$	Perturbation method, $Pr = 0{\cdot}72$, heat transfer from semi-infinite plate
Bandrowski & Rybski (1976)	0·5598	$\frac{1}{5}$	Similarity solution, $Sc = 2{\cdot}5$, surface molar fraction 5×10^{-4}, mass transfer from semi-infinite plate
Ackroyd (1976)	0·6361	$\frac{1}{5}$	Similarity solution, $Pr = 0{\cdot}72$, heat transfer from an infinite strip
	0·6026	$\frac{1}{5}$	Similarity solution, $Pr = 0{\cdot}72$, heat transfer from a square
Zakerullah & Ackroyd (1979)	0·5775	$\frac{1}{5}$	Similarity solution, $Pr = 0{\cdot}72$, heat transfer from a disk
Kerr (1980)	0·6883	$\frac{1}{5}$	Analogy solution, $Sc = 2{\cdot}5$, surface molar fraction 5×10^{-4}, mass transfer from a semi-infinite plate
Present numerical solution	0·609	0·203	Finite difference method, $Pr = 0{\cdot}7$, heat transfer from an infinite strip, $40 < Ra < 8 \times 10^3$
	0·621	$\frac{1}{5}$	Force the correlation to a $\frac{1}{5}$ power

TABLE 3. Theories on simple plate with buoyancy outward normal to its active surface (geometry 0) (laminar boundary-layer flow was assumed in all prior theories)

were similar to those calculated by boundary-layer theory. The measured heat transfer is about 19% higher than the integral solution of the boundary-layer equations.

Analytical solutions for geometry I are listed in table 5. A similarity solution seems unreasonable for this geometry. Wagner (1956), Clifton & Chapman (1969), Singh, Birkebak & Drake (1969), Singh & Birkebak (1969) and Bandrowski & Rybski (1976) obtained integral solutions of the boundary-layer equations with different assumptions at the plate edges.

Publications on the influence of extensions at plate edges are scarce. Restrepo & Glicksman (1974) examined three boundary conditions at the edge of a downward-facing heated plate. The heat-transfer rate is highest for the edge heated at plate temperature, lower for the edge maintained at room temperature, and lowest for the edge with extended insulation. Recently Hatfield & Edwards (1981) made holographic interferograms of downward-facing heated plates with adiabatic extension to side ratios from 0 to 0·2 for Rayleigh numbers between $1{\cdot}6 \times 10^4$ and $1{\cdot}6 \times 10^8$. Rather than a lengthscale of area/perimeter or 'hydraulic' diameter, they used aspect ratio as a separate parameter in their correlations for heat transfer both with and without an adiabatic extension.

Reference	$Nu = \text{C1}\ Ra^{\text{C2}}$ or $Sh = \text{C1}\ Ra_m^{\text{C2}}$ C1	C2	Range of Ra or Ra_m	Experimental technique
Fishenden & Saunders (1950)	0·51 0·46	0·19 $\frac{1}{5}$	8×10^3–5×10^5	Heated square plate in air, (present curve fit) Force the above correlation to $\frac{1}{5}$ power
Kadambi & Drake (1960)	0·613	$\frac{1}{5}$	Laminar	Heated circular plate in air
Bandrowski & Rybski (1976)	1·27 0·92	0·169 $\frac{1}{5}$	3×10^3–3×10^5	Rectangular naphthalene plate $Sc \approx 2{\cdot}5$ Force the above correlation to $\frac{1}{5}$ power
Birkebak & Abdulkadir (1970)	0·516	$\frac{1}{5}$	Laminar	Square plate in water
Fujii & Imura (1972)	0·440	$\frac{1}{5}$	$1{\cdot}25 \times 10^5$–$1{\cdot}25 \times 10^8$	Heated rectangular plate in air (Quasi-two-dimensional)
Aihara *et al.* (1972)	0·509 0·500	$\frac{1}{5}$ $\frac{1}{5}$	At $1{\cdot}62 \times 10^7$ At $0{\cdot}72 \times 10^7$	Heated rectangular plate in air (Quasi-two-dimensional)
Restrepo & Glicksman (1974)	0·445 0·31 0·52	$\frac{1}{5}$ $\frac{1}{5}$ $\frac{1}{5}$	$1{\cdot}6 \times 10^4$–$1{\cdot}6 \times 10^5$	Cooled edges, $T_{edge} = T_\infty$ Adiabatic extensions T edge $= T_s$ — Heated square plate in air
Present experiment	0·906 0·516 0·495	0·089 0·914 $\frac{1}{5}$	10–$2{\cdot}5 \times 10^2$ $2{\cdot}5 \times 10^2$–$4{\cdot}5 \times 10^3$	Square naphthalene plate in air, $Sc \approx 2{\cdot}5$ Force the correlation to $\frac{1}{5}$ power

TABLE 4. Experiments on simple plate with buoyancy inward normal to its source surface (geometry I).

2. Analysis

Consider steady laminar flow generated by a heated plate immersed in a large body of fluid (with a positive coefficient of thermal expansion). The plate is on the (X, Z)-plane, and the positive Y-axis is directed outward from the active surface. The governing equations with Boussinesq approximation can be written in dimensionless form as follows:

$$\left.\begin{aligned}
&\frac{\partial U}{\partial X}+\frac{\partial V}{\partial Y}+\frac{\partial W}{\partial Z}=0,\\
&U\frac{\partial U}{\partial X}+V\frac{\partial U}{\partial Y}+W\frac{\partial U}{\partial Z}=\frac{\partial^2 U}{\partial X^2}+\frac{\partial^2 U}{\partial Y^2}+\frac{\partial^2 U}{\partial Z^2}-\frac{\partial P}{\partial X},\\
&U\frac{\partial V}{\partial X}+V\frac{\partial V}{\partial Y}+W\frac{\partial V}{\partial Z}=\frac{\partial^2 V}{\partial X^2}+\frac{\partial^2 V}{\partial Y^2}+\frac{\partial^2 V}{\partial Z^2}-\frac{\partial P}{\partial Y}\pm Gr\Theta,\\
&U\frac{\partial W}{\partial X}+V\frac{\partial W}{\partial Y}+W\frac{\partial W}{\partial Z}=\frac{\partial^2 W}{\partial X^2}+\frac{\partial^2 W}{\partial Y^2}+\frac{\partial^2 W}{\partial Z^2}-\frac{\partial P}{\partial Z},\\
&U\frac{\partial \Theta}{\partial X}+V\frac{\partial \Theta}{\partial Y}+W\frac{\partial \Theta}{\partial Z}=\frac{1}{Pr}\left(\frac{\partial^2 \Theta}{\partial X^2}+\frac{\partial^2 \Theta}{\partial Y^2}+\frac{\partial^2 \Theta}{\partial Z^2}\right).
\end{aligned}\right\} \quad (1)$$

Reference	$Nu = C1\ Ra^{C2}$ or $Sh = C1\ Ra_m^{C2}$ C1	C2	Solution method
Wagner (1956)	0·50	$\frac{1}{5}$	Infinite strip, high Pr, boundary-layer thickness is assumed zero at plate edge, integral method, heat transfer
Clifton & Chapman (1969)	0·44	$\frac{1}{5}$	Infinite strip, $Pr = 0{\cdot}7$, boundary-layer thickness is assumed to be the hydrodynamic critical depth at plate edge, integral method, heat transfer
Singh *et al.* (1969)	0·50	$\frac{1}{5}$	For infinite strip; High Pr, boundary-layer thickness is assumed zero at plate edge, integral method with Ritz and Galerkin approximation, heat transfer
	0·543	$\frac{1}{5}$	For square plate
	0·484	$\frac{1}{5}$	For circular plate
Singh & Birkebak (1969)	0·460	$\frac{1}{5}$	Infinite strip, $Pr = 0{\cdot}7$, boundary-layer thickness is assumed minimum at plate edge, integral method, heat transfer
Bandrowski & Rybski (1976)	0·5269	$\frac{1}{5}$	Infinite strip, $Sc = 2{\cdot}5$, surface molar fraction 5×10^{-4}, boundary-layer thickness is assumed to be critical depth at plate edge, integral method, mass transfer
Present numerical solution	0·560	0·190	Finite-difference method, $Pr = 0{\cdot}7$, heat transfer from infinite strip, $40 < Ra < 8 \times 10^3$
	0·524	$\frac{1}{5}$	Force the correlation to $\frac{1}{5}$ power

TABLE 5. Theories on simple plate with buoyancy inward normal to its active surface (geometry I) (laminar boundary layer flow was assumed in all prior theories)

The dimensionless velocities are $U = ua/\nu$, $V = va/\nu$ and $W = wa/\nu$, corresponding to the dimensionless coordinates $X = x/a$, $Y = y/a$ and $Z = z/a$.

$$\Theta = (T - T_\infty)/(T_s - T_\infty)$$

is the dimensionless temperature; the dimensionless pressure is $P = p'a^2/\rho\nu^2$, where p' is the dynamic pressure, and the Grashof number $Gr = Ra/Pr$.

The sign of $Gr\,\Theta$ in the equation is positive when the heated plate is facing upward (0) and is negative when it is facing downward (I). Boundary conditions are $U = V = W = 0$, $\Theta = 1$ at the heated surface, $U = V = W = \partial\Theta/\partial T = 0$ at the insulated surface, and $U = V = W = \Theta = 0$ at infinity.

If the velocity components (U and W) parallel to the heated surface predominate it is reasonable to assume: (i) the diffusion of momentum, energy or mass in the horizontal direction is negligible compared with the corresponding convection term; and (ii) the vertical pressure gradient is due to buoyancy only.

A set of stretch variables that satisfy the above assumptions are

$$Y^* = Y Gr^{\frac{1}{5}}, \quad U^* = U Gr^{-\frac{2}{5}}, \quad V^* = V Gr^{-\frac{1}{5}}, \quad W^* = W Gr^{-\frac{2}{5}}, \quad P^* = P Gr^{-\frac{4}{5}}. \quad (2)$$

After substitution of stretch variables into (1) and simplification by comparison of the order of magnitude of terms, the three-dimensional boundary-layer equations are

written as

$$\left.\begin{aligned}
&\frac{\partial U^*}{\partial X}+\frac{\partial V^*}{\partial Y^*}+\frac{\partial W^*}{\partial Z}=0,\\
&U^*\frac{\partial U^*}{\partial X}+V^*\frac{\partial U^*}{\partial Y^*}+W^*\frac{\partial U^*}{\partial Z}=\frac{\partial^2 U^*}{\partial Y^{*2}}-\frac{\partial P^*}{\partial X},\\
&0=-\frac{\partial P^*}{\partial Y^*}\pm\Theta,\\
&U^*\frac{\partial W^*}{\partial X}+V^*\frac{\partial W^*}{\partial Y^*}+W^*\frac{\partial W^*}{\partial Z}=\frac{\partial^2 W^*}{\partial Y^{*2}}-\frac{\partial P^*}{\partial Z},\\
&U^*\frac{\partial\Theta}{\partial X}+V^*\frac{\partial\Theta}{\partial Y^*}+W^*\frac{\partial\Theta}{\partial Z}=\frac{1}{Pr}\frac{\partial^2\Theta}{\partial Y^{*2}}.
\end{aligned}\right\} \tag{3}$$

Boundary conditions are $U^* = V^* = W^* = 0$, $\Theta = 1$ at the heated surface, $U^* = V^* = W^* = \partial\Theta/\partial Y^* = 0$ at the insulated surface, and $U^* = \Theta = W^* = 0$ at infinity.

In (3), Gr is no longer a direct parameter of the problem but is hidden in the stretch variables. The solution of the equation will give

$$\left.\frac{\partial\Theta}{\partial Y^*}\right|_{Y^*=0} = f(Pr, X, Z). \tag{4}$$

From the definitions,

$$Nu(X,Z) = -\left.\frac{\partial\Theta}{\partial Y}\right|_{Y=0} = -Gr^{\frac{1}{5}}\left.\frac{\partial\Theta}{\partial Y^*}\right|_{Y^*=0}$$

$$= -Ra^{\frac{1}{5}}Pr^{-\frac{1}{5}}\left.\frac{\partial\Theta}{\partial Y^*}\right|_{Y^*=0}. \tag{5}$$

Therefore

$$Nu(X,Z) \propto Ra^{\frac{1}{5}} f'(Pr, X, Z). \tag{6}$$

The average Nusselt number, obtained by integration over the surface, is also proportional to Rayleigh number to the $\frac{1}{5}$ power.

Note that the use of the stretch variables indicates that if a laminar boundary-layer flow is induced by a horizontal heated surface with uniform temperature, Nu is proportional to $Gr^{\frac{1}{5}}$ or $Ra^{\frac{1}{5}}$ at a fixed Pr. With the same reasoning, the $\frac{1}{5}$-power law should extend to the analogous mass-transfer problem.

Various factors could invalidate (3) and cause a deviation from the $\frac{1}{5}$-power law. Vertical walls at the plate edges could replace the boundary-layer flow with a slow recirculating flow. For geometry 0 irregular plumes and turbulence are generated at high Rayleigh numbers. If the flow becomes turbulent, there are indications that the exponent would be $\frac{1}{3}$. For geometry I, the flow is stable and remains laminar at high Rayleigh numbers. The power-law correlations found in recent experimental studies are shown in table 4.

3. Finite-difference solution

For a heated plate infinite in the Z-direction (an infinite strip), the governing equations (1) can be reduced to a two-dimensional elliptic problem.

$$\left.\begin{aligned} \frac{\partial U}{\partial X}+\frac{\partial V}{\partial Y}&=0,\\ U\frac{\partial U}{\partial X}+V\frac{\partial U}{\partial Y}&=\frac{\partial^2 U}{\partial X^2}+\frac{\partial^2 U}{\partial Y^2}-\frac{\partial P}{\partial X},\\ U\frac{\partial V}{\partial X}+V\frac{\partial V}{\partial Y}&=\frac{\partial^2 V}{\partial X^2}+\frac{\partial^2 V}{\partial Y^2}-\frac{\partial P}{\partial Y}\pm Gr\,\Theta,\\ U\frac{\partial \Theta}{\partial X}+V\frac{\partial \Theta}{\partial Y}&=\frac{1}{Pr}\left(\frac{\partial^2 \Theta}{\partial X^2}+\frac{\partial^2 \Theta}{\partial Y^2}\right). \end{aligned}\right\} \tag{7}$$

Boundary conditions are

$$U = V = 0,\ \Theta = 1 \quad \text{at the heated surface,}$$

$$U = V = \partial\Theta/\partial Y = 0 \quad \text{at the insulated surface,}$$

and

$$U = V = \Theta = 0 \quad \text{at the domain boundary.}$$

Note that no boundary-layer assumptions have been made. Both the domain and the plate thickness are finite. There are several coordinate transformations to map the infinite domain into a finite one. However, these transformations usually lose the momentum and energy balance in the finite-difference equations. In the present solution method the domain is made sufficiently large and the plate sufficiently thin to achieve a desired accuracy. An expanding grid system is used for better efficiency in calculation.

The general finite-difference method comes from Patankar (1980). Details of the specific techniques for the present problem are given by Lau (1978). In the numerical scheme the calculation domain is discretized into rectangular control volumes. The convection and diffusion terms in the partial differential equations (7) are written in finite-difference form by the 'power-law scheme', which is an improved upwind-difference scheme. The pressure terms in the velocity equations are treated with the 'SIMPLE' algorithm, in which the variable pressure is iterated to satisfy continuity. Since the buoyancy term depends on the variable temperature, it is also subject to iteration. The finite-difference equations are solved by the 'line-by-line successive-relaxation method'. Owing to the nonlinearity of the problem, at high Rayleigh number and with a more complex geometry, the iteration has to be slowed down by smaller relaxation factors. The convergence criteria is set for a 1 % relative difference between two iteration steps in temperature calculations.

Figures 2(*a–f*) show the geometries of the six configurations in the present study as well as contours of constant temperature θ and stream function Ψ, which are described later. The dashed lines in the figures are the midplanes of the two-dimensional domain. The half-width of the heated surface is one unit. This surface is 11 units from the upper boundary, 3 units from the bottom, and its centre is 6 units from the side. The thickness of the heated surface, the insulation at the bottom, and the vertical walls are 0·1 unit. Since an infinitesimally thin insulation is impossible, the insulated edge in geometries 0 and I is 0·1 unit (that is, extension to plate width = $\frac{1}{20}$ on each side). The grid distance is small near the heated surface and the edge of the plate,

Ratio of the distances from the plate to the boundaries (upper: lower: side)	Nu	Relative difference (%)
11: 3: 6†	2·406	0
16: 5: 9	2·427	0·9
16: 5: 12	2·457	2·1
25: 5: 12	2·455	2·0

† Domain of present calculations as shown on figures 2(*a–e*).

TABLE 6. Effect of the domain size on the numerical solution for geometry 0. $Ra = 8 \times 10^2$; $Pr = 0{\cdot}7$; plate width = 2 units.

and expands gradually further away. A 14×19 grid system is used in the present (X, Y)-domain.

Since the heated surface is in the middle of the calculation domain, the boundary conditions at the plate surface cannot be prescribed directly. This difficulty is solved by assigning appropriate properties to the control volumes that represent the surfaces: $k_{\text{source}} = 10^6 k_{\text{fluid}}$ for the surface of uniform temperature; $k_{\text{insulation}} = 10^{-6} k_{\text{fluid}}$ for the insulated surface, and $\mu_{\text{solid}} = 7 \times 10^5 \mu_{\text{fluid}}$ for the solid surface, where k is thermal conductivity and μ is viscosity.

The partial differential equations (4) are elliptic. Physically, the flow is recirculating in the calculation domain. However, as the Rayleigh number increases, boundary-layer flow is expected near the heated surface. In such a flow, the fluid is largely modified by the heated surface and the immediate upstream condition. Therefore the solution of the present elliptic problem should exhibit the nature of local boundary-layer flow near the plate surface. Two characteristics of the local boundary-layer flow are relevant to the present solution method. First, because the boundary-layer thickness grows thinner at higher Rayleigh numbers, it is essential to have adequately small grid distance near the plate surface. Secondly, the domain boundary far from the heated plate can neither greatly affect the local flow patterns nor the heat transfer near the plate. Thus it is not necessary to use a large domain size to simulate the infinite domain as long as the local boundary-layer flow is developed. The influence of the domain size is shown in table 6. At $Ra = 800$, the heat transfer rate increases by 2% as the domain is approximately doubled. This influence should diminish at higher Ra.

Solutions are obtained for $Pr = 0{\cdot}7$ and $10 < Ra < 10^4$. Examples of isotherms and normalized stream functions are plotted on figure 2, while average Nusselt numbers are plotted as a function of Rayleigh number on figure 3. Isotherms are zero at the domain boundary, one at the heated surface. Stream functions are zero at the solid surface and maximum inside the largest recirculating loop.

Geometry 0

Figure 2(*a*) shows the solution for a heated plate facing upward. Particular attention is paid to the region near the plate. The fluid is drawn from the sides and below and increases its velocity near the plate edges. Then the fluid decelerates and turns upwards near the midplane. Finally, it attains a higher velocity in the plume. The average heat-transfer correlation obtained by least-square fit is $Nu = 0{\cdot}609 Ra^{0{\cdot}203}$ for $40 < Ra < 8 \times 10^3$. Forcing the correlation to a $\frac{1}{5}$ power law, $Nu \approx 0{\cdot}621 Ra^{\frac{1}{5}}$.

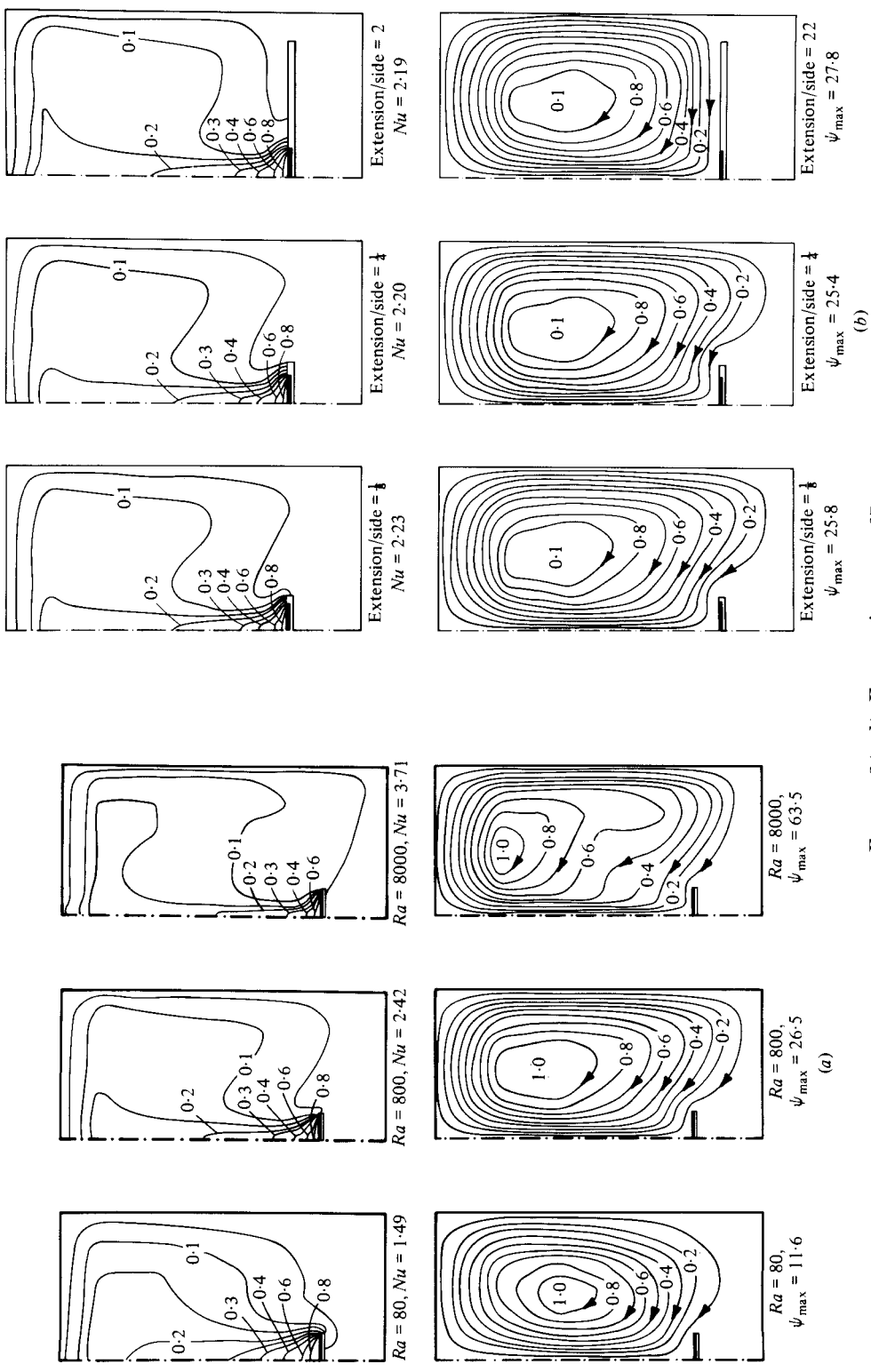

FIGURE 2 (*a*, *b*). For caption see p. 67.

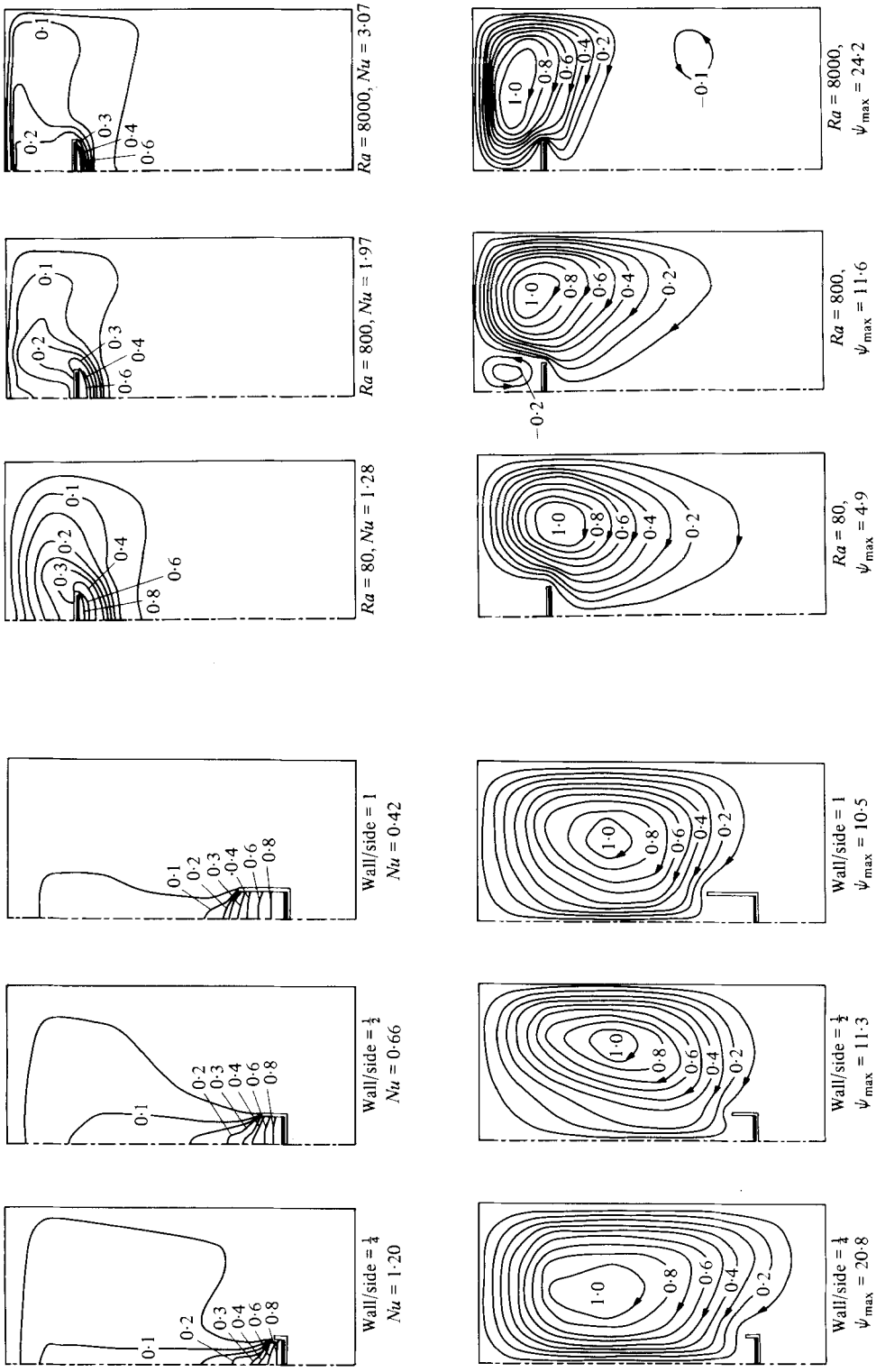

FIGURE 2 (*c*, *d*). For caption see facing page.

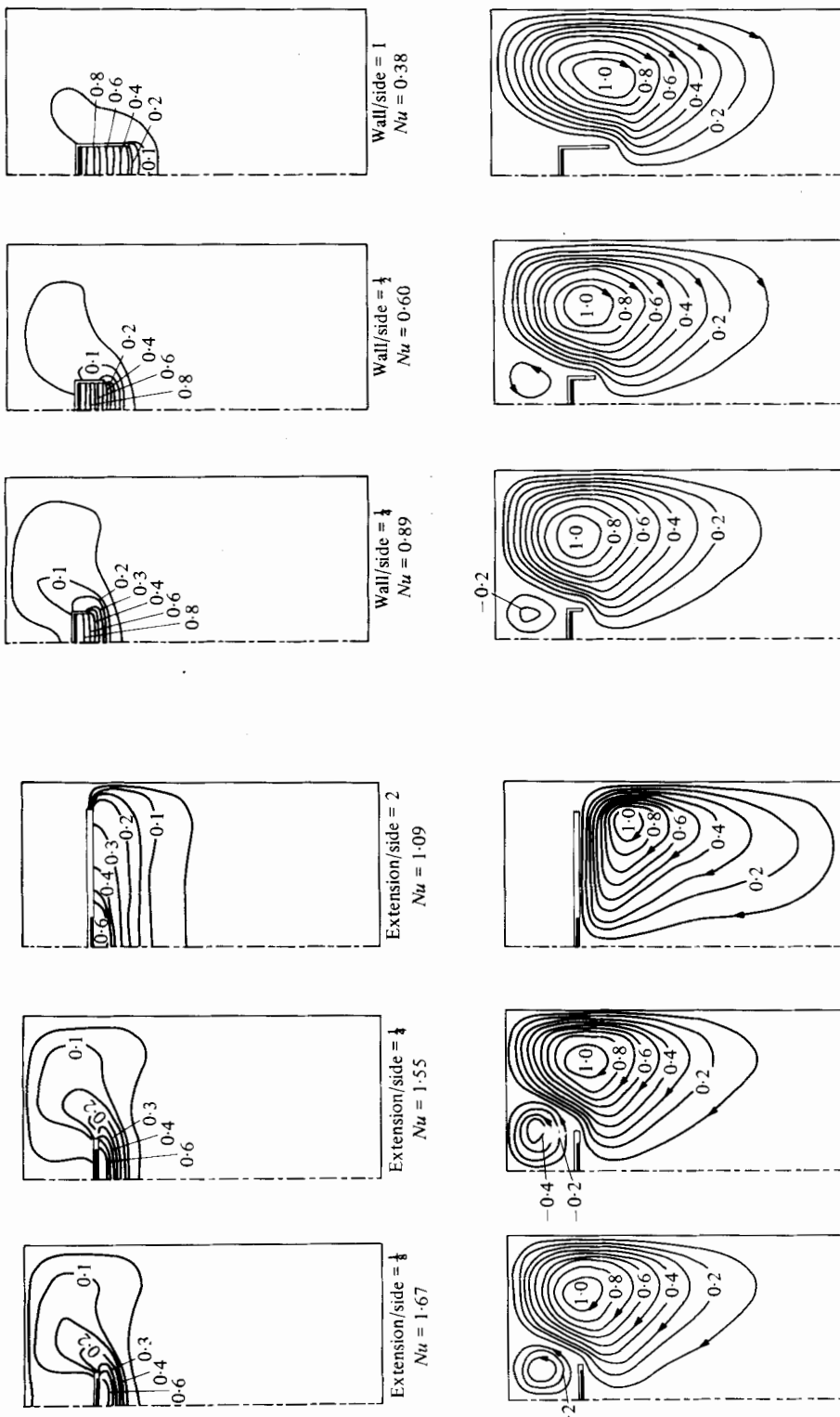

FIGURE 2. Isotherms Θ and normalized stream function Ψ/Ψ_{max} for (*a*) geometry 0 with $Pr = 0{\cdot}7$, $Ra = 80, 800, 8000$; (*b*) geometry 0H, $Pr = 0{\cdot}7$, $Ra = 800$; (*c*) geometry 0V, $Pr = 0{\cdot}7$, $Ra = 800$; (*d*) geometry 1, $Pr = 0{\cdot}7$, $Ra = 80, 800, 8000$; (*e*) for geometry 1H, $Pr = 0{\cdot}7$, $Ra = 800$; (*f*) geometry IV, $Pr = 0{\cdot}7$, $Ra = 800$.

Geometry 0H

Results for insulated horizontal extensions are shown in figure 2(*b*) for $Ra = 800$. The velocity of the approaching flow and the heat transfer are lower when the extensions are in place. In the present problem the driving force is generated by the active surface instead of the free stream. Therefore the boundary layer does not thicken indefinitely as the extension increases. The extension has a limited effect on the average heat transfer (figure 3*a*), which is probably approached near the maximum extension studied.

Geometry 0V

Since the flow with an upward-facing heated surface comes from the sides toward its centre, vertical walls at the edges block the flow and cause flow separation. Figure 2(*c*) shows that the convection pattern is moved above the top of the walls while the overall flow strength (indicated by Ψ_{max}) is reduced. The flow between the walls is relatively slow. Isotherms approximate a conduction pattern as the height of the wall increases. The heat transfer is considerably lowered by what is in effect a layer of thermal resistance on the heated surface.

Geometry I

Figure 2(*d*) represents the natural convection flow near a heated plate facing downward at different *Ra*. Fluid is drawn from below and turns parallel to the surface before flowing out past the edge. Velocity and temperature patterns of boundary-layer type can be observed near the heated surface. Compared to geometry 0, the flow is slower and the heat transfer is smaller. A curve fit of the present result is $Nu = 0{\cdot}560Ra^{0{\cdot}190}$ for $40 < Ra < 8 \times 10^3$ or $Nu \approx 0{\cdot}524Ra^{\frac{1}{5}}$.

Geometry IH

In geometry I fluid leaves the plate edges and forms a plume in the back of the plate. As shown on figure 2(*e*), the presence of an adiabatic extension obstructs the progress of the plume. The thermal boundary layer is extended along with the flow, and the heat transfer is lowered. The effect of the horizontal extension is much stronger in geometry IH (figure 3*b*) than in geometry 0H (figure 3*a*). The lower limit on heat transfer with a horizontal extension for geometry 0H has not been reached in the present study.

Geometry IV

A vertical wall has the same effect with geometry IV as with geometry 0V, but the flow stability is stronger and the fluid velocity slower. The near-conduction patterns between the walls shown in figure 2(*f*) indicate the predominance of the conduction mechanism on the heat-transfer process. The Nusselt number (cf. figure 3*b*) is low and almost independent of *Ra* for wall-to-side ratios of $\frac{1}{2}$ and 1 (or wall height to active plate half-width ratios of 1 and 2).

4. Experiment

Experiments are run in a sealed insulated room about 100 m^3 in volume. Inside the room a steel frame measuring $1{\cdot}5 \times 1{\cdot}5$ m^2 at the base and 2 m in height is covered with baffles at its top and upper parts. A naphthalene plate is hung below a balance inside the baffles. Sublimation takes place and the mass loss is measured by the balance. Since the test room is sealed during each experiment, the balance is remotely controlled. Thermocouples and barometers are also read from outside the room. The

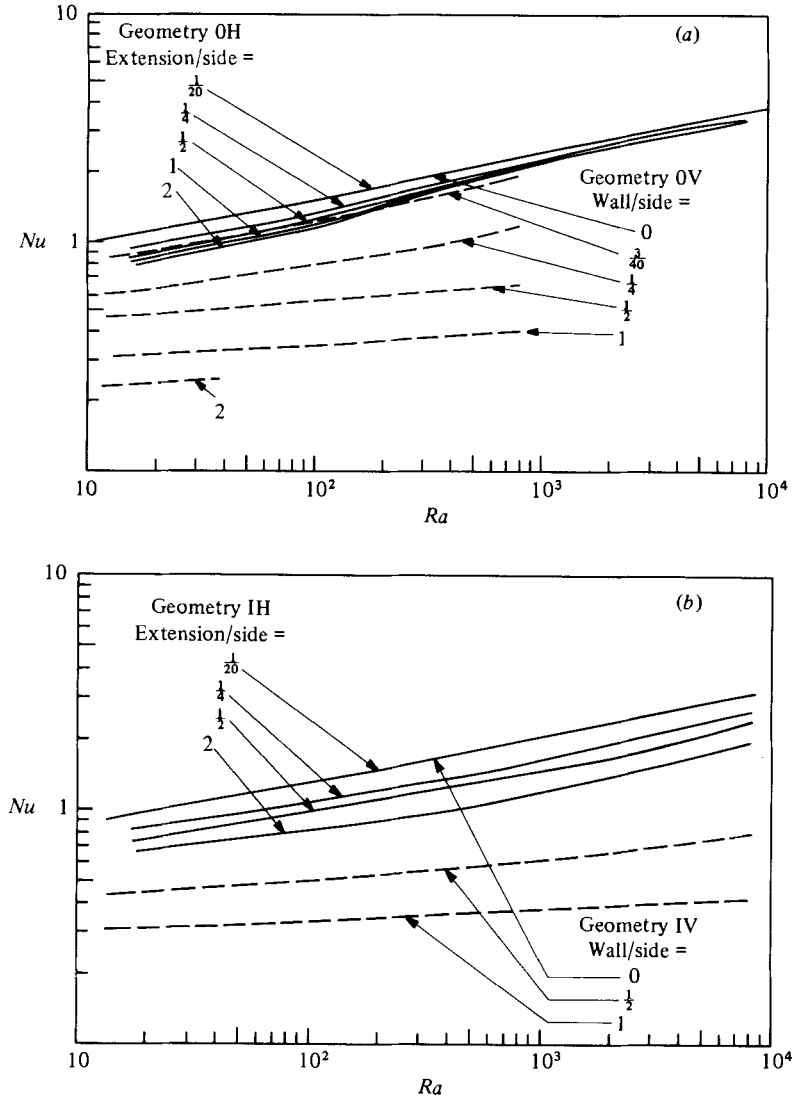

FIGURE 3. Average heat-transfer rate from a heated plate: (*a*) facing upward; (*b*) facing downward; numerical results.

mass-loss rate varies with the plate sizes and geometries and requires test durations ranging from an hour to a day.

The test plates are obtained by casting pure naphthalene in aluminium frames of different sizes. The sizes of the approximately square subliming surfaces varied from $2{\cdot}58 \times 2{\cdot}59$ cm^2 to $20{\cdot}30 \times 20{\cdot}29$ cm^2 and give a range of Ra_m from 10 to 10^4 at room temperature. Aluminium foils are added on the frames to make vertical walls. No actual horizontal extension is added to the naphthalene plate, but adhesive plastic tapes are used to cover the side edge and part of the naphthalene surface when a non-active horizontal extension is derived. Owing to the finite thickness of the aluminium frames, the extension-to-side ratio is not zero but less than 0·06 in the present experimental study of geometries 0 and I. The total weight of each sublimation plate is below 200 g. The mass loss can be measured by an analytical balance with a precision of $\pm 0{\cdot}05$ mg.

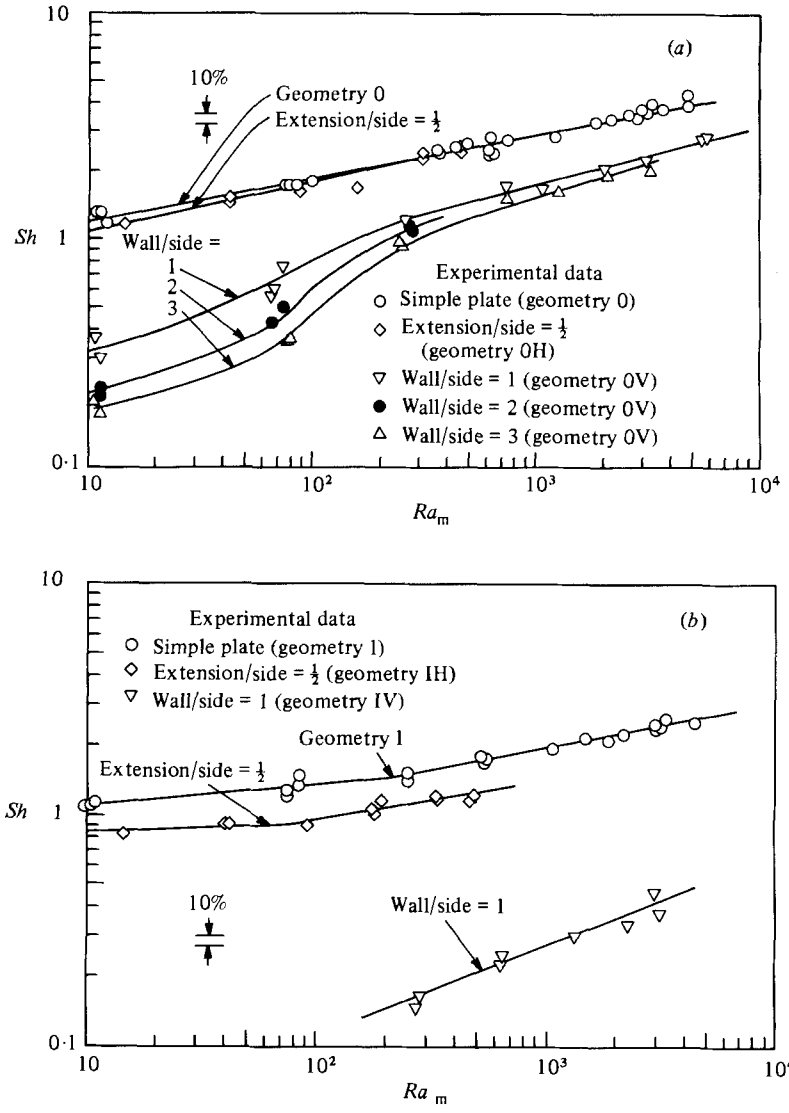

FIGURE 4. Average mass-transfer rate from a naphthalene plate (*a*) facing downward, (*b*) facing upward; experimental results.

As compared with heat-transfer experiments, the naphthalene-sublimation technique eliminates the serious problem of heat leakage by conduction and radiation. However, the sublimation of naphthalene would lower the temperature of the active surface slightly. Although this decrease in temperature is too small to be detected by thermocouples in the present experiment, it can create a thermal Rayleigh number. The natural-convection Rayleigh number induced by the sublimation latent heat is calculated to be a maximum of about 8 % of that due to the mass transfer.

Experimental results for a naphthalene plate facing downward (geometry 0) are shown on figure 4(*a*). The curve fit of the data is $Sh = 0{\cdot}766 Ra_m^{0{\cdot}195}$ ($\pm 10\,\%$) for $10 < Ra_m < 4{\cdot}8 \times 10^3$ or $Sh \approx 0{\cdot}746 Ra_m^{\frac{1}{5}}$.

No significant change in the mass-transfer rate is observed when horizontal extensions of half of the side are added. The effect of the vertical wall is large, but

diminishes as Ra_m increases. For a wall-to-side ratio of 1, Sh is lowered by about 70 % at $Ra_m = 10^2$ and 40 % at $Ra_m = 10^3$.

Figure 4 (*b*) shows the experimental results for a naphthalene plate facing upward (geometry I). The curve fit is $Sh = 0{\cdot}906 Ra_m^{0{\cdot}089}$ for $10 < Ra_m < 2{\cdot}5 \times 10^2$ and $Sh = 0{\cdot}516 Ra_m^{0{\cdot}194}$ for $2{\cdot}5 \times 10^2 < Ra_m < 4{\cdot}5 \times 10^3$. For the results with a higher Rayleigh-number range the equations can be forced to a $\frac{1}{5}$ power and become $Sh \approx 0{\cdot}495 Ra_m^{\frac{1}{5}}$ for $2{\cdot}5 \times 10^2 < Ra_m < 4{\cdot}5 \times 10^3$. For geometry IH with the extension-to-side ratio of $\frac{1}{2}$, the mass-transfer rate is lowered by a factor of about 20 % over a wide range of Ra_m. For geometry IV with a wall-to-side ratio of unity, the decrease of the mass-transfer rate is very large – about 85 % at $Ra_m = 10^3$.

5. Comparison of results

The present numerical solutions for infinite horizontal strips and experimental results for square surfaces can be compared with other analyses and experiments. Some basic points should be noted before comparing results.

(i) Mass transfer is analogous to the heat-transfer problem only if the velocity of the fluid at the active surface is small. This condition is well satisfied in the present naphthalene experiments.

(ii) Sh is analogous to Nu and Sc is analogous to Pr. The parameter Pr or Sc varies widely in different studies. Pr is about 0·7 for air; and Sc is approximately 2·5 in the naphthalene–air system and 2200 in some electrochemical experiments. The present numerical study indicates that at a fixed Ra, as Pr increases from 0·7 to 2·5, Nu increases by 7·5 % in geometry 0 and 5·0 % in geometry I. This result agrees with the boundary-layer analysis in Pera & Gebhart (1973), predicting that Nu increases with Pr to the $\frac{1}{20}$ power at fixed Ra for $1 < Pr < 10$. When Pr approaches infinity, the Nu–Ra correlation is independent of Pr.

(iii) The characteristic length (active area/perimeter) is useful in comparing results for plates of different shapes. This may also be inferred from the analytical results of Ackroyd (1976) and Zakerullah & Ackroyd (1979) in table 3 for geometry 0, and Singh *et al.* (1969*a*) in table 5 for geometry I.

(iv) The present numerical method takes advantage of the local boundary-layer flow near the heated surface in the elliptic problem. A relatively small calculation domain is used to simulate an infinite environment. However, when the flow is slow and the conduction mechanism is strong, the problem is highly dependent on the domain size. Since the test room in the experiment is much larger than the calculation domain in the numerical solution, comparison between the two results is inadequate for the slow-flow situation when the Rayleigh number is low or the vertical walls are added.

Experimental results for geometry 0 are summarized in table 2. Heat-transfer and electrochemical experiments are usually performed at higher Ra than are naphthalene experiments. Bosworth (1952), Mikheyev (1968) and Al-Arabi (1976) give the same $\frac{1}{4}$ power heat-transfer correlation and agree reasonably well with electrochemical experiments by Lloyd (1974). Wragg (1968) and Wragg & Loomba (1970). In a lower range of Ra, the data of naphthalene experiments by Goldstein *et al.* (1973) and Bandrowski & Rybski (1976) are close if they are put into a $\frac{1}{5}$ power correlation.

As shown in table 3, solutions of the boundary-layer equation for geometry 0 are in good agreement. The present numerical solution includes the non-boundary-layer nature near the centre and the edge of the plate. The resultant Nusselt number is slightly lower than those found with the boundary-layer analysis.

Comparison of some representative results for outward buoyancy is made in figure 5(*a*). The present mass-transfer experimental results are about 20 % greater than the calculation of the finite-difference solution. The $\frac{1}{4}$ power correlation from Wragg & Loomba (1970) intersects the present experimental $\frac{1}{5}$ power correlation around $Ra = 10^3$. Extrapolation of other experimental results may also do so at Ra between 10^3 to 10^4.

The natural convection flow with geometry 0 is unstable. The critical Ra observed for the transition from laminar flow for $Pr = 0{\cdot}7$ is 7×10^5, found by Rottem & Claassen (1969), $3{\cdot}6 \times 10^5$, found by Pera & Gebhart (1973), and $3{\cdot}8 \times 10^4$, found by Ishigura *et al.* (1978). In reality, the three-dimensional effect in a finite plate may lower the critical Ra further. Both the present experimental and numerical results suggest that the $\frac{1}{5}$ power does exist for Ra between 10 and 10^4. When the downstream flow becomes unstable or it begins a transition to turbulent flow, the power of the Nu–Ra correlation will increase gradually from $\frac{1}{5}$ to perhaps $\frac{1}{3}$.

The edge effects on geometries 0H and 0V from the present study are compared in figure 5(*a*). The decrease of the heat-transfer rate (with a horizontal extension-to-side ratio of $\frac{1}{2}$) is 10 % in the numerical result, but much smaller in the experiment. Effects of vertical walls are shown for wall-to-side ratios of 1 and 2. However, the comparison is inadequate, probably due to the finite domain size in the slow-flow situation in the numerical calculations.

The fluid flow induced in geometry I is stable and no turbulent flow has been observed. Results of different experiments – Birkebak & Abdulkadir (1970), Fujii & Imura (1972) and Aihara *et al.* (1972) – agree well and are shown in table 4. The present experiment, covering the lower range of Ra, is close to the extrapolated results of others. Prior integral solutions of the boundary-layer equations (Wagner 1956; Clifton & Chapman 1969; Singh *et al.* 1969; Singh & Birkebak 1969) do not differ much, even though the assumptions of the boundary condition at the plate edge are different. The present numerical result is approximately 6 % above the experiment and within 10 % of the other theories shown in table 5.

Figure 5(*b*) shows some representative results for the case of inward buoyancy. In geometry IH, for a horizontal extension-to-side ratio of $\frac{1}{2}$, the present numerical and experimental results both indicate a lowering of the transfer rate by 20 %. Restrepo & Glicksman (1974) found 30 % for a ratio of $\frac{5}{14}$ in their heat-transfer experiments. The Hatfield & Edwards (1981) study on the effect of small horizontal extensions shows the same trend as the present study. In geometry IV, the effects of a vertical wall are large, as shown in both the numerical prediction and the experiment. However, detailed comparison is inadequate as the domain used in the calculation is much smaller than that used in the experiment.

6. Conclusions

Compiling the results of prior and present studies, several conclusions are made.

(i) Despite the plume formation, the laminar boundary-layer flow seems to exist near the active surface in either geometry 0 or I. For Ra between 10 and 10^4, a $\frac{1}{5}$ power law is generally found for the Nusselt-number or Sherwood-number variation. In geometry I, the experiments indicate a somewhat lower exponent at Rayleigh numbers below 100.

(ii) The insulated horizontal extension causes a limited reduction in the transfer rate in geometry 0H, but is much more effective in geometry IH.

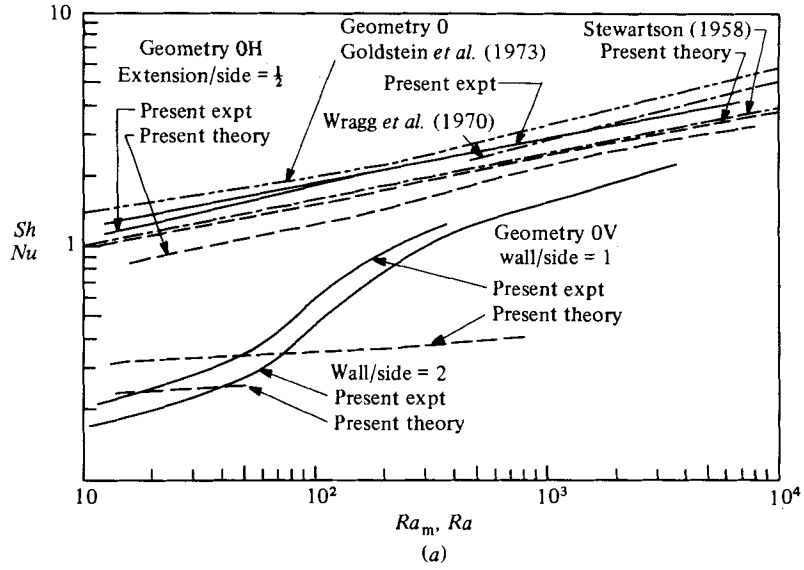

FIGURE 5. Comparison of the heat- and mass-transfer results: (*a*) for outward buoyancy and (*b*) for inward buoyancy.

(iii) The insulated vertical wall lowers the transfer rate significantly in geometry 0V and can cause an even larger reduction in geometry IV. The relative reduction tends to be smaller at higher Rayleigh numbers.

This study was supported by the National Science Foundation under Grant NSF/ENG 77-21626.

REFERENCES

ACKROYD, J. A. D. 1976 Laminar natural convection boundary layers on near-horizontal plates. *Proc. R. Soc. Lond.* A 352, 249.

AIHARA, T., YAMADA, Y. & ENDO, E. 1972 Free convection along the downward-facing surface of a heated horizontal plate. *Int. J. Heat Mass Transfer* **15**, 2335.

AL-ARABI, M. & EL-RIEDY, M. K. 1976 Natural convection heat transfer from isothermal horizontal plates of different shapes. *Int. J. Heat Mass Transfer* **19**, 1399.

BANDROWSKI, J. & RYBSKI, W. 1976 Free convection mass transfer from horizontal plates. *Int. J. Heat Mass Transfer* **19**, 827.

BIRKEBAK, R. C. & ABDULKADIR, A. 1970 Heat transfer by natural convection from the lower side of finite horizontal heated surface. *Preprint, 4th Intl Heat Transfer Conf., Paris*, 4, NC 2-2.

BOSWORTH, R. L. C. 1952 *Heat Transfer Phenomena.* Wiley.

CLIFTON, J. V. & CHAPMAN, A. J. 1969 Natural convection on a finite-size horizontal plate. *Int. J. Heat Mass Transfer* **12**, 1573.

FAW, R. E. & DULLFORCE, T. A. 1981 Holographic interferometry measurement of convective heat transfer beneath a heated horizontal plate in air. *Int. J. Heat Mass Transfer* **24**, 859.

FISHENDEN, M. & SAUNDERS, O. A. 1950 *An Introduction to Heat Transfer.* Oxford University Press.

FUJII, T. & UMURA, H. 1972 Natural convection heat transfer from a plate with arbitrary inclination. *Int. J. Heat Mass Transfer* **15**, 755.

GOLDSTEIN, R. J., SPARROW, E. M. & JONES, D. C. 1973 Natural convection mass transfer adjacent to horizontal plates. *Int. J. Heat Mass Transfer* **16**, 1025.

HATFIELD, D. W. & EDWARD, D. K. 1981 Edge and aspect ratio effects on natural convection from the horizontal heated plate facing downwards. *Int. J. Heat Mass Transfer* **24**, 1019.

ISHIGURO, R., ABE, T., NAGASE, H. & NAKANISHI, S. 1978 Heat transfer and flow stability of natural convection over upward-facing horizontal surfaces. *In Proc. 6th Intl Heat Transfer Conf.* vol. 2, p. 229.

KADAMBI, V. & DRAKE, R. M. 1960 Free convection heat transfer from horizontal surfaces for prescribed variation in surface temperature and mass flow through the surface. *Tech. Rep. Mech. Engng*, HT-1, *Princeton University.*

KERR, C. N. 1980 Analogy solution of free convection mass transfer from downward-facing horizontal plates. *Int. J. Heat Mass Transfer* **23**, 247.

LAU, K. S. 1978 The effect of edge conditions on laminar natural convection adjacent to a horizontal plate. M.S. thesis, University of Minnesota.

LEVY, S. & SCHENECTADY, N. Y. 1955 Integral method in natural convection flow. *J. Appl. Mech.* **77**, 515.

LLOYD, J. R. & MORAN, W. R. 1974 Natural convection adjacent to horizontal surfaces of various planforms. *Trans. A.S.M.E.* C: *J. Heat Transfer* **96**, 443.

MIKHEYEV, M. 1968 *Fundamentals of Heat Transfer.* Mir.

PATANKAR, S. V. 1980 Numerical heat transfer and fluid flow. Hemisphere.

PERA, L. & GEBHART, B. 1973 Natural convection boundary layer flow over horizontal and slightly inclined surfaces. *Int. J. Heat Mass Transfer* **16**, 1131.

RESTREPO, F. & GLICKSMAN, L. R. 1974 The effect of edge conditions on natural convection from a horizontal plate. *Int. J. Heat Mass Transfer* **17**, 135.

ROTEM, Z. & CLAASSEN, L. 1969 Natural convection above unconfined horizontal surfaces. *J. Fluid Mech.* **39**, 173.

SINGH, S. N., BIRKEBAK, R. C. & DRAKE, R. M. 1969 Laminar free convection heat transfer from downward-facing horizontal surfaces of finite dimensions. *Adv. Heat Mass Transfer* **2**, 87.

SINGH, S. N. & BIRKEBAK, R. C. 1969 Laminar free convection from a horizontal infinite strip facing downwards. *Z. angew. Math. Phys.* **20**, 454.

STEWARTSON, K. 1958 On the free convection from horizontal plates. *Z. angew. Math. Phys.* **9**, 276.

WAGNER, C. 1956 Discussion of 'Integral method in natural convection flow' by S. Levy. *J. Appl. Mech.* **78**, 320.

WRAGG, A. A. 1968 Free convection mass transfer at horizontal electrodes. *Electrochim. Acta* **13**, 2159.

WRAGG, A. A. & LOOMBA, R. P. 1970 Free convection flow patterns at horizontal surfaces with ionic mass transfer. *Int. J. Heat Mass Transfer* **13**, 439.

ZAKERULLAH, M. & ACKROYD, J. A. D. 1979 Laminar natural convection boundary layers on horizontal circular discs. *Z. angew. Math. Phys.* **30**, 427.